Isothermal melt crystallization and melting behaviour of syndiotactic polypropylene†

Pitt Supaphol,[1]* Joseph E Spruiell[2] and Jar-Shyong Lin[3]
[1]Petroleum and Petrochemical College, Chulalongkorn University, Bangkok 10330, Thailand
[2]Materials Science and Engineering, University of Tennessee, Knoxville, TN 37996, USA
[3]Solid State Division, Oak Ridge National Laboratory, Oak Ridge, TN 37831, USA

Abstract: The lamellar morphological information and subsequent melting behaviour of syndiotactic polypropylene (s-PP) samples isothermally crystallized at crystallization temperatures ranging from 30 to 95 °C have been investigated using a combination of wide-angle X-ray diffraction (WAXD), small-angle X-ray scattering (SAXS) and differential scanning calorimetry (DSC) techniques. Three known methods for determining the equilibrium melting temperature T_m°, namely the Gibbs–Thomson extrapolation, the linear Hoffman–Weeks extrapolation and the non-linear Hoffman–Weeks extrapolation, have been employed to evaluate this important thermodynamic parameter, and the results obtained are compared. Finally, an estimate of the equilibrium melting temperature for a perfect s-PP sample $(T_m^\circ)_{100\%}$ is given.
© 2000 Society of Chemical Industry

Keywords: syndiotactic polypropylene; isothermal crystallization; lamellar morphology; lamellar thickness; melting behaviour; equilibrium melting temperature

INTRODUCTION

The syndiotactic form of polypropylene (s-PP) was first synthesized in the early 1960s by Natta and co-workers[1,2] based on Ziegler–Natta catalysis, but the resulting polymer contained too many regio-irregular defects (eg head-to-head/tail-to-tail type defects) despite a fair level of syndiotactic content. A much improved s-PP was successfully synthesized in 1988 by Ewen *et al*[3] who reported that highly stereo-regular and regio-regular s-PP can be polymerized using a novel metallocene catalysis. The new catalytic systems have made it possible to produce s-PP with much improved purity and yields, which led to renewed interest in both scientific research (eg Rogriguez-Arnold *et al*[4]) and industrial applications.[5–10]

Studies related to the crystallization process of semicrystalline polymers are of great importance in polymer processing, because the resulting physical properties are strongly dependent on the morphology formed and the extent of crystallization. It is therefore very important to understand the processing–structure–property inter-relationships of the studied materials. Investigations concerning the chain conformation, crystal structure, morphology and phase transitions in s-PP have been reported extensively in recent years. These studies up to 1994 were reviewed and discussed in a publication by Rodriguez-Arnold *et al.* [4] Studies on the subject of isothermal crystallization of s-PP include the Avrami kinetics of the crystallization process,[11–13] the kinetics of the linear growth rates,[12,14,15] and the morphology of the single crystals.[16]

In this work, wide-angle X-ray diffraction (WAXD) and small angle X-ray scattering (SAXS) techniques were employed to determine lamellar morphological information of s-PP samples isothermally crystallized at various temperatures. Differential scanning calorimetry (DSC) was used to study the melting behaviour of these samples.

EXPERIMENTAL DETAILS

Materials

The s-PP resin (ie s-PP#4) used in this study was synthesized using a metallocene catalyst and was produced commercially in pellet form by Fina Oil and Chemical Co of La Porte, Texas. Molecular characterization data show the following molecular weight information: $M_n = 81\,300\,\mathrm{g\,mol^{-1}}$, $M_w = 171\,000\,\mathrm{g\,mol^{-1}}$, $M_z = 294\,000\,\mathrm{g\,mol^{-1}}$, and $M_w/M_n = 2.1$. In addition, the syndiotacticity measured by ^{13}CNMR shows the racemic dyad content [%*r*] to be 89.2%, the racemic triad content [%*rr*] to be 84.4%, and the racemic pentad content [%*rrrr*] to be 74.6%. The glass transition temperature T_g was determined to be about -6 °C.[13]

* Correspondence to: Pitt Supaphol, Petroleum and Petrochemical College, Chulalongkorn University, Bangkok 10330, Thailand
E-mail: ps@sunsv1.ppc.chula.ac.th
† Parts of this work were presented at the 2nd Asia/Australia Regional Meeting of the Polymer Processing Society (PPS) held in Bangkok, Thailand during 1–3 December 1999.
(*Received 17 September 1999; revised version received 11 April 2000; accepted 12 May 2000*)

© 2000 Society of Chemical Industry.

Sample preparation

Sliced pellets were melt-pressed at a pressure of about 4.6×10^2 MN m^{-2} between a pair of polyimide films, which in turn were sandwiched between a pair of thick metal plates in a Wabash compression moulding machine, the temperature of which was preset at 190 °C. After 10 min holding time, a film of about 290 μm thickness was taken out and allowed to cool to room temperature at ambient conditions between the two metal plates. This treatment assumes that previous thermomechanical history was essentially erased and provides a standard crystalline memory condition for our experiments. The samples used in this study were cut from the as-prepared film, placed between two clean glass slides, brought to melt in a Mettler hot-stage at a fusion temperature T_f of 190 °C for 5 min to ensure complete melting,[17] and then quickly brought to crystallize isothermally in another Mettler hot-stage calibrated to ±0.5 °C in the crystallization temperature T_c range 30–95 °C. After complete crystallization at T_c the samples were quenched in liquid nitrogen to prevent further change in crystallinity due to residual thermal energy. Finally, WAXD, SAXS and DSC measurements were performed on these samples.

Wide-angle X-ray diffraction

The WAXD technique was employed to determine the crystal modification and the apparent degree of crystallinity in the samples prepared. The WAXD intensity patterns were collected on a Rigaku–Denki diffractometer (CuK_α radiation, $\lambda = 1.54$ Å) equipped with a computerized data collection and analytical system. The operating condition of the X-ray source was set at a voltage of 35 kV and a current of 40 mA.

Small-angle X-ray scattering

The SAXS intensity data of the samples prepared were measured on the ORNL 10-m SAXS apparatus,[18] which consists mainly of a pinhole-collimated CuK_α X-ray source ($\lambda = 1.54$ Å) operating at 80 mA and 40 kV, and a 20×20 cm^2 two-dimensional position-sensitive detector with each virtual cell element about 3 mm apart. A sample-to-detector distance of 5.12 m was used. The scattered intensity was stored in a 64×64 data array. Corrections were made for instrumental backgrounds, dark current due to cosmic radiation and electronic noises, and detector non-uniformity and efficiency (via an Fe^{55} radioactive standard which emits γ-rays isotropically) on a cell-by-cell basis. The intensity data were azimuthally averaged at each scattering vector $q = (4\pi/\lambda)\sin(\theta/2)$ (where λ and θ are the X-ray wavelength and the scattering angle, respectively) ranging from 0.058 to 1.004 nm^{-1}, and were converted to an absolute differential scattering cross-section by means of pre-calibrated secondary standards.[19]

Differential scanning calorimetry

A Perkin-Elmer DSC-7 differential scanning calorimeter was used to record subsequent melting thermograms of the samples prepared. All of the melting thermograms were recorded using a scanning rate of 20 °C min^{-1}. Temperature calibration was performed using a pure indium standard ($T_m^\circ = 156.6$ °C and $\Delta H_f^\circ = 28.5$ J g^{-1}). The consistency of the temperature calibration was checked every other run to ensure reliability and accuracy of the data obtained.

RESULTS

Figure 1 illustrates WAXD diffractograms for s-PP samples isothermally crystallized in a Mellter hot-stage at $T_c = 30$, 40, 50, 60, 70, 80, 85, 90 and 95 °C. Apparently, the characteristic crystalline peaks are present at the scattering angles $2\theta = 12.18 \pm 0.03°$, $15.93 \pm 0.03°$, 20.64 0.11° and 24.56 0.04°. By consulting all the publications dedicated to crystallographical studies of s-PP,[20–34] we strongly believe that the results shown in Fig 1 can be best described by the limit-disordered form I[26,28,30] (after the most recent nomenclature given by De Rosa *et al*[35]), which has an orthorhombic unit cell with axes $a = 14.5$ Å, $b = 5.6$ Å and $c = 7.4$ Å and exhibits an antichiral packing of chains only along the a axis (see Fig 1B in ref 35). The space group proposed for this crystal modification was *Pcaa*.[21,27] According to this unit cell, the characteristic X-ray peaks are observed at $2\theta = 12.2°$, 15.8°, 20.8° and 24.5°, corresponding to d-spacing at 7.25, 5.60, 4.27 and 3.63 Å, and to reflection planes at (200), (010), (111) and (400), respectively.

WAXD patterns not only indicate to us the crystal modification formed in these samples, but they also suggest the apparent degree of crystallinity χ^{WAXD} these samples possess. Intuitively, the WAXD degree of crystallinity χ^{WAXD} can be determined from the WAXD patterns based on the ratio of the integrated intensities under the crystalline peaks A_c to the integrated total intensities A_t (ie $A_t = A_c + A_a$, where

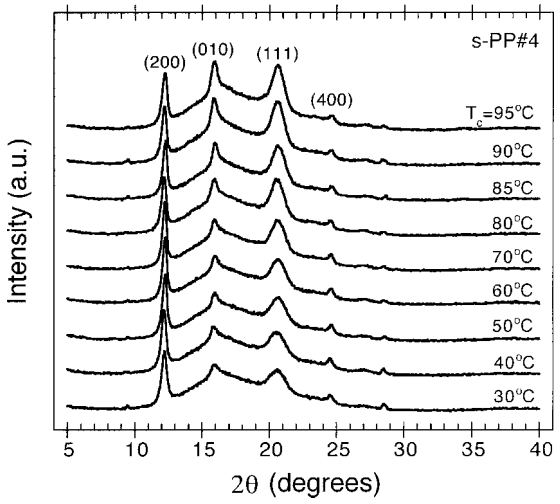

Figure 1. WAX diffractograms of s-PP#4 samples isothermally crystallized at various temperatures T_c from 30 to 95 °C.

Table 1. Experimental values of the WAXD degree of crystallinity χ_c^{WAXD}, the maximum scattering vector q_{max}, the long period L_B, the lamellar thickness l_c and the melting temperature T_m

T_c (°C)	χ_c^{WAXD}	q_{max} (nm^{-1})	L_B (nm)	l_c (nm)	T_m (°C)
30	0.28	0.649	9.7	2.7	–
40	0.28	0.618	10.2	2.8	106.0±0.4
50	0.30	0.586	10.7	3.2	107.1±0.2
60	0.30	0.561	11.2	3.3	108.8±0.2
70	0.29	0.533	11.8	3.4	112.1±0.6
80	0.31	0.512	12.3	3.8	116.5±0.7
85	0.33	0.508	12.4	4.1	118.5±0.7
90	0.34	0.501	12.5	4.2	120.8±0.5
95	0.33	0.498	12.6	4.2	123.3±0.7

A_a is the integrated intensities under the amorphous halo), ie

$$\chi_c^{WAXD} = \frac{A_c}{A_c + A_a} \in [0, 1] \quad (1)$$

Qualitatively, an increase in size of the crystalline scattering peaks with increasing crystallization temperature (see Fig 1) suggests to us that the WAXD degree of crystallinity χ_c^{WAXD} is an increasing function of crystallization temperature, at least within the temperature range studied. The quantitative results are summarized in Table 1 and will be discussed further in the next section.

Figure 2 shows azimuthally averaged SAXS profiles collected on these samples. The raw data are plotted in Fig 2 as different geometrical dots, while solid lines drawn through each set of data represent smoothened profiles. The Lorentz-corrected SAXS intensity profiles (ie Kratky plots) of the experimental SAXS intensity profiles (see Fig 2) are shown in Fig 3. With an assumption of a two-phase system comprising crystalline and amorphous fractions with sharp interfaces, the average value of the long period L_B of the lamellar morphology (hereafter called the long period L_B) can be estimated from the maximum value of the scattering vector q_{max} observed in the Lorentz-corrected SAXS scattering profiles (see Fig 3). According to the Bragg law and the mathematical definition of the scattering vector q, the long period L_B can then be calculated from the equation

$$L_B = \frac{2\pi}{q_{max}} \quad (2)$$

According to Fig 3, the fact that q_{max} decreases with increasing crystallization temperature indicates that the long period L_B increases with increasing crystallization temperature. The quantitative results are summarized in Table 1 and will be discussed further in the next section.

Figure 4 illustrates the melting behaviour of these samples during a DSC heating scan (20 °C min^{-1}). For

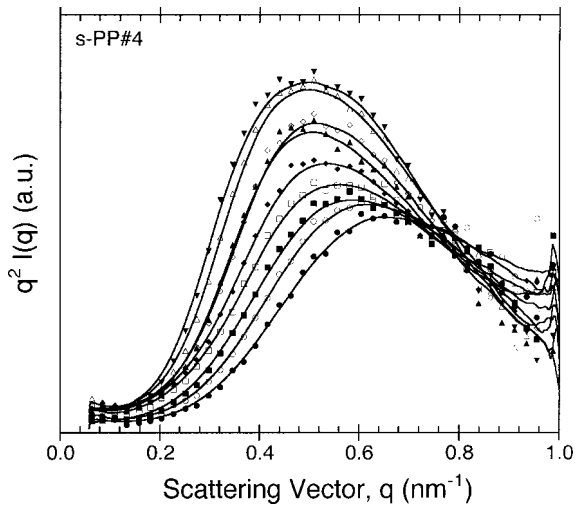

Figure 3. Lorentz-corrected SAXS profiles (Kratky plots) of s-PP#4 samples isothermally crystallized at various temperatures T_c ranging from 30 to 95 °C (see Fig 2 for key).

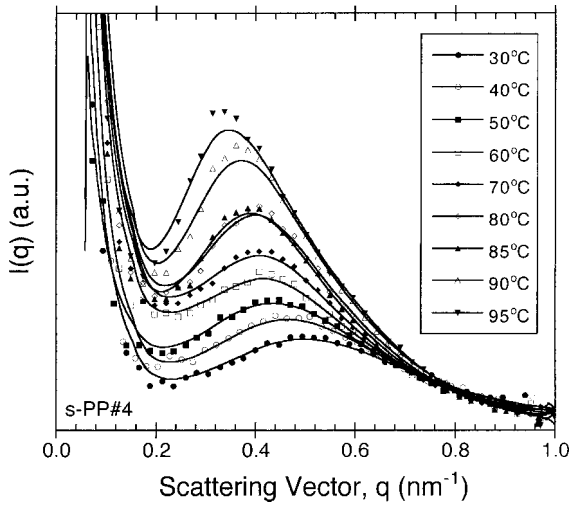

Figure 2. Azimuthally averaged SAXS profiles of s-PP#4 samples isothermally crystallized at various temperatures T_c from 30 to 95 °C.

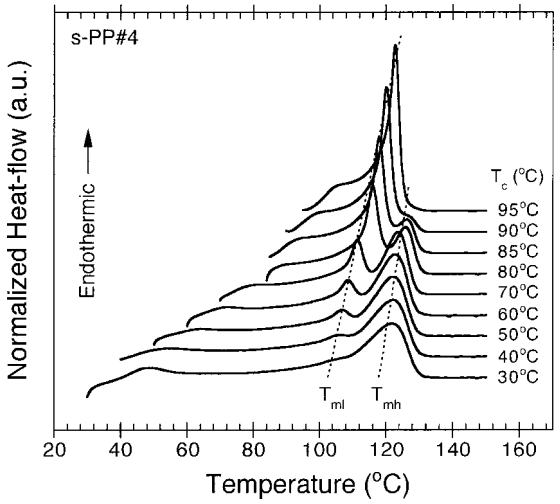

Figure 4. Subsequent melting thermograms observed in DSC using a heating rate of 20 °C min^{-1} for s-PP#4 samples isothermally crystallized at various temperatures T_c from 30 to 95 °C.

samples isothermally crystallized at $T_c \leq 90\,^{\circ}C$, three melting endotherms are observed, while only two melting endotherms are present in the sample isothermally crystallized at $T_c = 95\,^{\circ}C$. According to our recent work,[36] the minor endotherm (the peak temperature of which is denoted in ref 36 as the minor peak temperature T_l) located close to the corresponding crystallization temperature T_c, represents the melting of the secondary crystallites formed at T_c. The low-temperature melting endotherm (the peak temperature of which is denoted in ref 36 as the low-melting peak temperature T_{ml}) corresponds to the melting of the primary crystallites formed at T_c, while the high-temperature melting endotherm (the peak temperature of which is denoted in ref 36 as the high-melting peak temperature T_{mh}) is attributed to the melting of the crystallites recrystallized during a heating scan. Thus, the triple-melting behaviour of s-PP observed in subsequent melting endotherms in DSC may be best described as the contributions from: (i) melting of the secondary crystallites and their recrystallization, (ii) partial melting of the less stable fraction of the primary crystallites and their recrystallization; (iii) melting of the primary crystallites; and lastly (iv) remelting of the recrystallized crystallites formed during the heating scan.

At this point, one may question the integrity of the T_{ml} values corresponding to peak temperatures, obtained from DSC scans at $20\,^{\circ}C\,min^{-1}$, of the melting endotherms of primary crystallites formed at T_c. As a first approximation, the apparent melting temperature should vary with the heating rate used because it should affect the positions of maxima (or minima) of the corresponding melting and re-crystallization processes. We have previously demonstrated[36] that, for samples isothermally crystallized at $T_c = 75$ and $95\,^{\circ}C$, the apparent melting temperatures of the primary crystallites (T_{ml}) were not greatly affected by changes in the heating rate used, even though a very slight increase with increasing heating rate was observed (eg for samples isothermally crystallized at $75\,^{\circ}C$, $T_{ml} = 113.3\,^{\circ}C$ when the heating rate used was $5\,^{\circ}C\,min^{-1}$, whereas $T_{ml} = 114.0\,^{\circ}C$ when it was $20\,^{\circ}C\,min^{-1}$), presumably a result of the superheating effect. Based on this observation, it is legitimate to conclude that the peak temperatures of the melting endotherms of primary crystallites (T_{ml}) obtained from DSC scans at $20\,^{\circ}C\,min^{-1}$ are credible and reliable, and these peak values will be further analysed accordingly.

DISCUSSION

Table 1 summarizes values of the WAXD degree of crystallinity χ_c^{WAXD}, the maximum scattering vector q_{max}, the long period L_B and the melting (peak) temperature of the primary crystallites formed at the corresponding T_c (ie the peak temperature of the low-temperature melting endotherm $T_{ml} = T_m$). If the assumption of the two-phase system is valid for describing the lamellar morphology of s-PP samples isothermally crystallized within the temperature range studied, the thickness of mature crystals l_c (lamellar thickness) can be evaluated as the multiplication product of the WAXD degree of crystallinity and the long period, ie

$$l_c = L_B \chi_c^{WAXD} \tag{3}$$

The lamellar thicknesses l_c calculated using eqn (3) are also summarized in Table 1. It is apparent, according to Table 1, that the degree of crystallinity χ_c^{WAXD}, the long period L_B, the lamellar thickness l_c and the melting temperature T_m are all found to increase with increasing crystallization temperature, at least within the temperature range studied. This is because crystals formed at high crystallization temperatures T_c are more stable (thicker) than those formed at lower T_c. Because the lamellar thickness l_c of the primary crystals formed at a given T_c has a definite relationship with the observed melting temperature T_m of these crystals according to the Gibbs–Thomson equation.[37]

$$T_m = T_m^{\circ}\left(1 - \frac{2\sigma_e^{GT}}{\Delta H_f^{\circ}} \cdot \frac{1}{l_c}\right) \tag{4}$$

where T_m° is the equilibrium melting temperature (ie the melting temperature of the crystalline lamellae of infinite thickness), σ_e^{GT} is the interfacial free energy for forming the basal plane of mature crystals and ΔH_f° is the equilibrium enthalpy of fusion for the crystalline phase, the observed melting temperature of the primary crystals is then expected to increase with increasing crystallization temperature T_c. It is worth mentioning that eqn (4) is valid only for lamellae whose lateral dimensions (ie the width of the growth fronts) are much larger than their thickness, which we believe is true for s-PP.

According to eqn (4), the equilibrium melting temperature T_m° of the polymer of interest may be evaluated more accurately by extrapolating a plot of the observed melting temperature T_m versus the reciprocal value of the lamellar thickness l_c^{-1} (ie T_m versus l_c^{-1} plot) to $l_c^{-1} = 0$, at which point the y-intercept is taken as the value of the equilibrium melting temperature T_m°. Figure 5 shows a Gibbs–Thomson plot of the observed T_m–l_c^{-1} data summarized in Table 1. The bulk of the data were fitted to a linear curve-fitting procedure and are given by (ie the line $T_m(l_c^{-1})$)

$$T_m(l_c^{-1}) = 166.3 - \frac{189.2}{l_c} \qquad (r^2 = 0.979) \tag{5}$$

It should be noted that the units of T_m and l_c are °C and nm, respectively. Accordingly, eqn (5) gives us the value of the equilibrium melting temperature T_m^{GT} (ie $T_m(l_c^{-1} \to 0)$) to be $166.3 \pm 0.5\,^{\circ}C$ (data points at $T_c = 30$, 40 and $50\,^{\circ}C$ are excluded from the extrapolation on the basis that the low-temperature melting endotherms are not well resolved).

According to eqn (4), the basal interfacial free

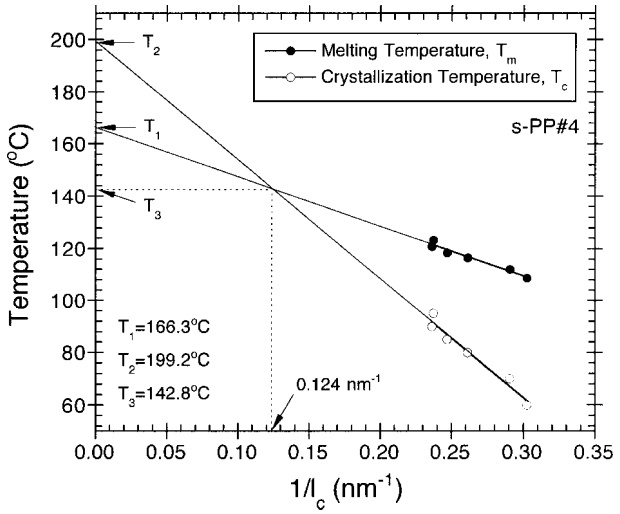

Figure 5. Relations between the inverse lamellar thickness l_c^{-1}, the observed melting temperature T_m, and the crystallization temperature T_c obtained for s-PP#4 samples isothermally crystallized at various temperatures T_c from 60 to 95°C. T_1 represents $T_m(l_c^{-1} \rightarrow 0)$, T_2 represents $T_c(l_c^{-1} \rightarrow 0)$, and T_3 represent T_m^{LHW}.

energy σ_e^{GT} can also be evaluated from the slope of the line $T_m(l_c^{-1})$ (see eqn 5), provided that the value of the equilibrium enthalpy of fusion ΔH_f° is known *a priori*. In principle, the value of the equilibrium enthalpy of fusion ΔH_f° can be estimated from the observed enthalpy of fusion ΔH_f and a knowledge of the degree of crystallinity, ie

$$\Delta H_f^\circ = \frac{\Delta H_f}{\chi_c^{WAXD}} \qquad (6)$$

In this case, we have chosen the enthalpy of fusion of the sample crystallized at $T_c = 95°C$ (ie $\Delta H_f = 36.5 \pm 0.2\,J\,g^{-1}$) based on the fact that the enthalpic contribution from the melting of the crystals recrystallized during the heating scan is minimal compared to samples crystallized at lower temperatures. According to eqn (6), the equilibrium enthalpy of fusion ΔH_f° for this particular s-PP resin is then found to be about $109.3 \pm 0.5\,J\,g^{-1}$ or $4.6\,kJ\,mol^{-1}$, and finally gives us the value of the basal interfacial free energy σ_e^{GT} as about $57.8 \pm 0.3\,mJ\,m^{-2}$.

Analogous to the apparent linear relationship in the plot of the observed T_m–l_c^{-1} data, a plot of the crystallization temperature T_c as a function of the reciprocal value of the lamellar thickness l_c^{-1}, also shown in Fig 5, clearly demonstrates that a linear relationship in the T_c–l_c^{-1} data is also observed. Clearly, the bulk of the data can be described by a linear relationship similar to the line $T_m(l_c^{-1})$ (as dictated by eqn (4)). When curve-fitting the bulk of the data to a linear relationship similar to that exhibited in eqn (5), the following equation (ie the line $T_c(l_c^{-1})$) is obtained:

$$T_c(l_c^{-1}) = 199.2 - \frac{454.6}{l_c} \qquad (r^2 = 0.981) \qquad (7)$$

Again, the units of T_c and l_c are °C and nm, respectively. Although the line $T_c(l_c^{-1})$ does not have theoretical support at this point (even though the relationship between T_c and l_c may be described to some extent by eqn (10)), some interesting experimental observations related to the relationship between the lines $T_c(l_c^{-1})$ and $T_m(l_c^{-1})$ have to be addressed.

First, a crossing of the lines $T_c(l_c^{-1})$ and $T_m(l_c^{-1})$ at a finite lamellar thickness (ie $l_c^{T_m=T_c} = 8.1$ nm) is evident in Fig 5. By referring to the linear Hoffman–Weeks extrapolation method[38] (see later), the crossing of the lines $T_c(l_c^{-1})$ and $T_m(l_c^{-1})$ gives us nothing else but the value of the equilibrium melting temperature T_m° according to this method (ie $T_m^{LHW} = 142.8°C$). Clearly, this value is much lower than that obtained from the Gibbs–Thomson extrapolation (ie $T_m^{GT} = 166.3°C$ versus $T_m^{LHW} = 142.8°C$). The fact that the T_m^{LHW} value was found at a finite value of the lamellar thickness led Schmidtke *et al*[39] to suggest that the T_m^{LHW} value only represents the temperature at which point the crystal growth mechanism is free from the kinetic effects such that perfect crystals are immediately formed. Based on this notion, the T_m^{LHW} value obtained from the linear Hoffman–Weeks procedure does not necessarily represent the true equilibrium melting temperature T_m° of the polymer of interest, but may be taken as a lower limit (ie $T_m^\circ > 142.8°C$ for this particular s-PP resin).

Secondly, it was shown in a recent work by Hauser *et al*[40] that the relationship between the crystallization temperature T_c and the reciprocal value of the lamellar thickness l_c^{-1}, in the form of the line $T_c(l_c^{-1})$, for s-PP and syndiotactic poly(propene-*co*-octene) (s-P(P-*co*-O)) samples of varying defect contents fall on a common line (see Fig 12 in ref 40 or Fig 1 in ref 41). They found that the extrapolation of the common line $T_c(l_c^{-1})$ to $l_c^{-1} = 0$ gives a value (ie $T_c(l_c^{-1} \rightarrow 0) \neq 193°C$ according to eqn (31) in ref 39) approaching that of the equilibrium melting temperature T_m° of a perfect s-PP (ie $(T_m^\circ)_{100\%} = 196°C$[39,40]). Surprisingly, extrapolation of our T_c–l_c^{-1} data to $l_c^{-1} = 0$ suggests the value of $T_c(l_c^{-1} \rightarrow 0)$ to be 199.2°C, which is very close to the value given by Schmidtke *et al.*[39] Comparison of eqn (7) which describes the relationship of the T_c–l_c^{-1} data of our s-PP resin with eqn (31) in ref 39 which describes the relationship of the T_c–l_c^{-1} data of s-PP and s-P(P-*co*-O) resins used in ref 40, suggests to us that our data line up extremely well on the common line $T_c(l_c^{-1})$ shown in Fig 12 in ref 40 or Fig 1 in ref 41, with our T_c–l_c^{-1} data being very comparable to those of the s-P(P-*co*-O)15 sample which has a comparable amount of total defects to our s-PP sample (ie 9.4% (mol of total defects) in s-P(P-*co*-O)15 versus 11.8% (mol of *meso* defects) in our sample).

Let us now pay closer attention to the relationship between the observed melting temperature T_m and the crystallization temperature T_c. Two methods have been proposed to describe the observed T_m–T_c data,

and obtain the equilibrium melting temperature T_m° of the polymer of interest as a result. These methods are (i) the *linear* Hoffman–Weeks extrapolation (LHW, see eqn (8)),[38] and (ii) the *non-linear* Hoffman–Weeks extrapolation (NLHW).[42]

In the LHW extrapolation method, if l_c^{cr} denotes the critical lamellar thickness as dictated in the classical Lauritzen–Hoffman secondary nucleation theory (the LH secondary nucleation theory),[37] to prevent the growing crystal from melting at its own crystallization temperature T_c the average initial lamellar thickness l_c^* has to be some number (δl_c) greater than the critical lamellar thickness. This results in the average initial lamellar thickness l_c^* observed at an arbitrary T_c being in the form

$$l_c^* = \frac{2\sigma_e^{LH}}{\Delta f} + \delta l_c \approx \frac{2\sigma_e^{LH} T_m^\circ}{\Delta H_f^\circ \Delta T} + \delta l_c \qquad (8)$$

where Δf is the free enthalpy per unit volume of the crystal, σ_e^{LH} is the interfacial free energy for forming the basal plane of initial crystals, and δl_c is a quantity related to very small thickening of the crystals and is a very weak function of temperature.

If the thickening behaviour of the crystals can be expressed by an introduction of the thickening ratio $\beta^{LHW} = l_c/l_c^* \geq 1$ (for a coherent two-dimensional nucleation process), the observed melting point T_m of a crystal which has been thickened by a factor β^{LHW} can be expressed by

$$T_m = T_m^\circ\left(1 - \frac{2\sigma_e^{LH}}{\Delta H_f^\circ} \cdot \frac{1}{\beta^{LHW} l_c^*}\right) \qquad (9)$$

In the case where β^{LHW} equals unity and δl_c equals zero (ie non-thickening), the basal interfacial free energy given in eqn (4)(σ_e^{GT}) should be equivalent to that appearing in eqn (9)(σ_e^{LH}) and the crystals growing at an arbitrary crystallization temperature T_c will melt simulateneously (ie $T_m = T_c$); thus eqn (9) becomes

$$T_c = T_m^\circ\left(1 - \frac{2\sigma_e^{LH}}{\Delta H_f^\circ} \cdot \frac{1}{l_c^*}\right) \qquad (10)$$

Based on eqns (9) and (10), Hoffman and Weeks[38] were able to derive a very useful equation which allows determination of the equilibrium melting temperature T_m° from a series of the observed melting temperatures T_m of crystals crystallized at crystallization temperatures T_c:

$$T_m = \frac{T_c}{2\beta^{LHW}} + T_m^\circ\left[1 - \frac{1}{2\beta^{LHW}}\right] \qquad (11)$$

According to eqn (11), linear extrapolation of observed T_m–T_c data to the line $T_m = T_c$ yields the equilibrium melting temperature T_m° value, and yields the thickening ratio β^{LHW} from the slope. This type of plot is hereafter referred to as the LHW extrapolation. The factor 2 in eqn (11) suggests that the thickness of the crystals undergoing melting is approximately double that of the initial critical thickness.

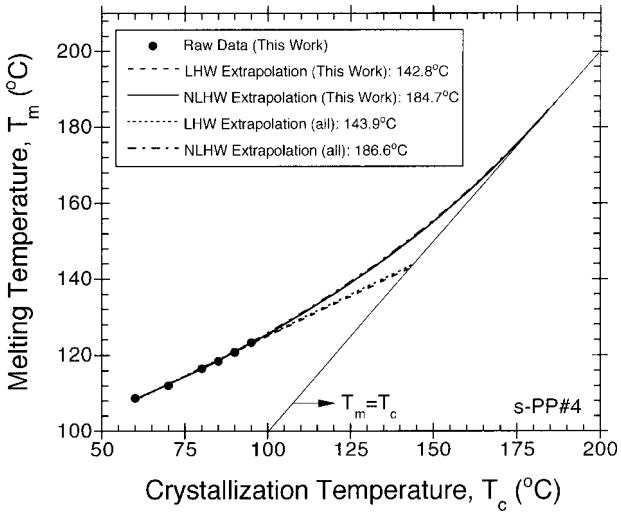

Figure 6. Plot of the observed melting temperature T_m as a function of the crystallization temperature T_c (without the data points at T_c=30, 40 and 50°C). The dashed line is the linear Hoffman–Weeks extrapolation based on experimental data points (●). The solid line is the non-linear Hoffman-Weeks extrapolation calculated using β^m=1, a=2.34 and T_m^{NLHW} = 184.7°C. The dotted line is the linear Hoffman–Weeks extrapolation based on experimental data of this work (●) and those reported earlier in refs 13 and 36 (not shown). The dashed-dotted line is the non-linear Hoffman-Weeks extrapolation calculated using β^m=1, a=2.25 and T_m^{NLHW} = 186.6°C.

We have carried out the LHW extrapolation on our observed T_m–T_c data listed in Table 1 and show the result in Fig 6. According to the extrapolation, the equilibrium melting temperature as suggested by this method is found to be $T_m^{LHW} = 142.8$°C with the thickening ratio β^{LHW} and the correlation coefficient of the fit r^2 being 1.2 and 0.998, respectively (see dashed line in Fig 6). If two other sets of the observed T_m–T_c data (which we measured earlier using DSC; see Table 4 in ref 13 and Table 1 in ref 36) are included in the extrapolation, the resulting values of T_m^{LHW}, β^{LHW} and r^2 are respectively found to be 143.9°C, 1.2 and 0.998 (see dotted line in Fig 6). The fact that the difference in the two T_m^{LHW} values is only about 1°C suggests to us that the data collected in this work and the other two reports are satisfactorily reliable and accurate.

We have mentioned previously that the equilibrium melting temperature suggested by the LHW extrapolation method (T_m^{LHW}) does not represent the true equilibrium melting temperature T_m° of the polymer of interest, because it was shown in our case that the T_m^{LHW} value was found at a finite value of the lamellar thickness (ie $l_c^{T_m-T_c} = 8.1$ nm). Moreover, Marand *et al*[42] recently demonstrated using high density polyethylene (HDPE) as the model system that the accuracy of the T_m^{LHW} value to the true equilibrium melting temperature T_m° depends significantly on the range of the observed T_m–T_c data. The closer this range is to the true equilibrium melting temperature T_m°, the better is the accuracy of the T_m^{LHW} value

obtained. In practice, however, the closer the range of the observed T_m–T_c data is to the true equilibrium melting temperature T_m°, the more extensive the lamellar thickening process becomes, especially in the cases of flexible semi-crystalline polymers which exhibit significant α relaxation (eg HDPE, isotactic polypropylene (i-PP)).

In HDPE, the lamellar thickening process is responsible for the curvature observed in the observed T_m–T_c data when they are collected over a wide enough temperature range and, according to Alamo *et al*,[43] these data can be divided into three regions. The first region corresponds to the lowest crystallization temperature range, within which the thickness of the crystallites is less sensitive to changes in T_c; therefore the observed T_m is essentially only slightly dependent on T_c. The second region corresponds to the highest crystallization temperature range within which prolonged crystallization time is needed to allow for the completion of the crystallization process; during this time period, the initial nuclei can undergo excessive thickening even before the bulk reaches 5–10% crystallinity.[43] The extent of the thickening process is a function of both time and crystallization temperature. The third region corresponds to the temperature range intermediate to both extremes. In this range, linearity in the plot of observed T_m versus T_c is evident, and it is the region to which the LHW procedure is usually applied.

Even though Alamo *et al*[43] provided to some extent an explanation on the curvature observed in the T_m–T_c data, they did not provide a solution to cope with this experimental fact. Recently, Marand *et al*[42] have been able to provide a theoretical explanation for the curvature observed in the T_m–T_c data collected over a wide temperature range and a convincing demonstration of the new theory on HDPE which they have chosen as their model system. In addition, the theory provides a new method for determining the equilibrium melting temperature T_m° of the polymer of interest from the observed T_m–T_c data. This method is hereafter called the non-linear Hoffman–Weeks (NLHW) extrapolation. Recently, Xu *et al*[44] successfully applied the NLHW extrapolative procedure to obtain an equilibrium melting temperature T_m° of Ziegler–Natta catalysed i-PP of around 212 °C.

Based on the proposition made by Lauritzen and Passaglia[45] on stem length fluctuations during chain folding, the basal interfacial free energy associated with a nucleus of critical size σ_e^{LP} accounting for the extra lateral surface free energy due to fold protrusion and for the mixing entropy associated with stems of different lengths can be expressed as a function of undercooling as

$$\sigma_e^{LP} = \sigma_e^1(1 + \zeta \Delta T) \qquad (12)$$

where σ_e^1 is the interfacial energy associated with the basal plane of the initial crystals and can be estimated from the slope of l_c^* versus ΔT^{-1},[37,46] and ζ is a temperature coefficient of roughly $0.0025\,K^{-1}$ estimated for the case of HDPE.[37,46] In the case of fold protrusion, the basal interfacial free energy σ_e^{LH} as given in eqn (8) needs to be corrected with σ_e^{LP}, which results in the average initial lamellar thickness being in the form

$$l_c^* = \frac{2\sigma_e^1 T_m^\circ}{\Delta H_f^\circ \Delta T} + \frac{2\sigma_e^1 \zeta T_m^\circ}{\Delta H_f^\circ} + \delta l_c = \frac{D_1}{\Delta T} + D_2 \qquad (13)$$

where D_1 and D_2 are constants, and all other parameters are the same as previously defined. Equation (13) is able to explain the discrepancy between the thickening parameter measured experimentally (D_2 in eqn (13)) and that calculated based on the previous theoretical postulation (δl_c in eqn (8)).[42]

Combination of eqns (4), (12) and (13) led Marand *et al*[42] to propose a new method, the so-called NLHW extrapolation, for the analysis of observed T_m–T_c data based on the equation of the form

$$\frac{T_m^\circ}{T_m^\circ - T_m} = \beta^m \frac{\sigma_e^1}{\sigma_e^{GT}} \left[\frac{T_m^\circ}{T_m^\circ - T_c} + \frac{D_2 \Delta H_f^\circ}{2\sigma_e^1} \right] \qquad (14a)$$

or in a simpler form

$$M = \beta^m \frac{\sigma_e^1}{\sigma_e^{GT}} (X + a) \qquad (14b)$$

where β^m is the thickening ratio and has the same phisical meaning as β^{LHW} used earlier, and all other parameters are the same as previously defined. It is worth noting that for most cases it is safe to assume that $\sigma_e^1 \approx \sigma_e^{GT} \approx \sigma_e^{LH}$.[42] Precautionary remarks for using the NLHW procedure were addressed in detail in the original publication by Marand *et al.*[42]

To apply eqn (14) for analysing the experimental T_m–T_c data in real polymer systems, the observed T_m data need to be collected from samples crystallized at different temperatures but having the same lamellar thickening coefficient β^m. For each set of the observed T_m–T_c data, corresponding values of M and X in eqn (14) can be calculated for a given choice of the equilibrium melting temperature T_m°. For the case of $\sigma_e^1 \approx \sigma_e^{GT}$, the true equilibrium melting temperature T_m° is taken as the seed T_m° value which results in the plot of M versus X being a straight line with a slope of unity (ie $\beta^m = 1$) and an intercept of a (ie $a = D_2 \Delta H_f^\circ / 2\sigma_e^1$). Because we have shown previously that lamellar thickening does not occur in s-PP during isothermal crystallization, at least within the temperature range studied, it is reasonable to assume that the observed T_m data summarized in Table 1 were collected from lamellae having the same thickening coefficient β^m, thus enabling them to be analysed using this method.

Figure 7 shows variation of the M versus X, calculated from the data shown in Table 1 according to eqn (14), for different choices of the seed temperature. The equilibrium melting temperature as suggested by this method, T_m^{NLHW}, for this particular s-PP sample is found to be 184.7 °C (for

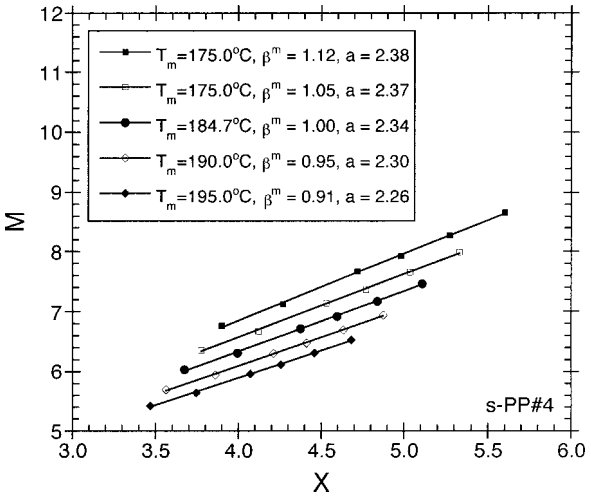

Figure 7. Plots of the scaled observed melting temperature $M = T_m^\circ/(T_m^\circ - T_m)$ against the scaled crystallization temperature $X = T_m^\circ/(T_m^\circ - T_c)$ for various choices of the seeded equilibrium melting temperature T_m° for the observed T_m–T_c data of this work (without the data points at T_c=30,40 and 50 °C).

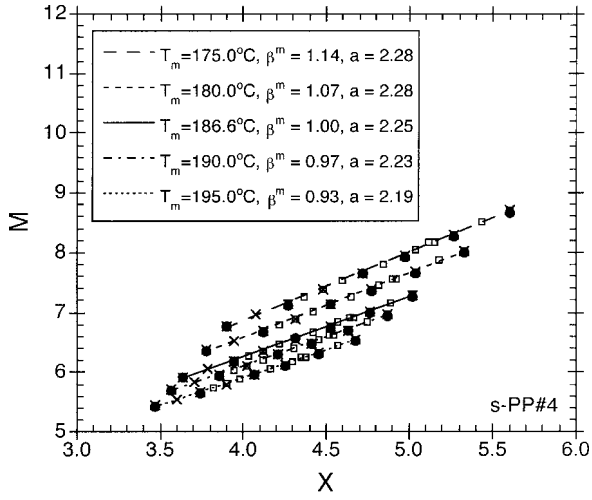

Figure 8. Plots of the scaled observed melting temperature $M = T_m^\circ/(T_m^\circ - T_m)$ against the scaled crystallization temperature $X = T_m^\circ/(T_m^\circ - T_c)$ for various choices of the seeded equilibrium melting temperature T_m° for the observed T_m–T_c data of this work (●) and those reported earlier in refs 13 (□) and 36 (×).

$\beta^m = 1$). The value of a associated with the resulting T_m° value can be determined from the y-intercept of the plot of M versus X and it is found to be 2.34. The NLHW extrapolation of the observed T_m–T_c data summarized in Table 1 is also shown in Fig 6 as the solid line. It should be noted that the correlation coefficient r^2 of the fit obtained for both methods suggests that the NLHW extrapolation gives a better fit to the set of the data than the LHW extrapolation (r^2=0.999 in NLHW versus r^2=0.998 in LHW).

Again, if we are to include in the extrapolation the two other sets of observed T_m–T_c data we measured earlier using DSC (see Table 4 in ref 13 and Table 1 in ref 36), the values of T_m^{NLHW}, a and r^2 which result in β^m being unity are respectively found to be 186.6 °C, 2.25 and 0.999. Plots of M versus X, calculated for all the data sets, for different choices of seed temperature are shown in Fig 8, while the resulting NLHW extrapolation is presented in plots shown in Fig 6 as the dashed-dotted line (raw data for the two other sets of data are not shown).

Finally, we would like to end our discussion with the observed temperature dependence of the initial lamellar thickness l_c^*. Because we have shown in our previous work[36] using DSC that the lamellar thickness of s-PP does not increase during crystallization, it is reasonable to assume that the initial lamellar thickness l_c^* is equivalent to the experimental values of the lamellar thickness l_c summarized in Table 1. This allows us to model the experimental data according to eqn (13). To use eqn (13) to fit the experimental data, *a priori* knowledge of the equilibrium melting temperature T_m° is required. In this work, we have shown that by using different methods to determine the equilibrium melting temperature T_m° four different values are obtained: (i) from the Gibbs–Thomson extrapolation method, $T_m^{GT} = T_m(l_c^{-1} \to 0) = 166.3$ °C; (ii) from the extrapolation of T_c–l_c^{-1} data to $l_c^{-1} = 0$, $T_c(l_c^{-1} \to 0) = 199.2$ °C; (iii) from the LHW extrapolation method, $T_m^{LHW} = 142.8$ °C; and (iv) from the NLHW extrapolation method, $T_m^{NLHW} = 184.7$ °C. Of the four values, only $T_m^{GT} = 166.3$ °C and $T_m^{NLHW} = 184.7$ °C have a solid theoretical basis, and either of the values can therefore be taken as the true equilibrium melting temperature T_m° of this particular s-PP resin. We do not, however, have an explanation for the discrepancy between the two values at present.

Figure 9 shows a plot of the lamellar thickness l_c as a function of crystallization temperature T_c (data points at T_c=30, 40 and 50 °C are excluded from the plot). According to the best fit for a given choice of the true equilibrium melting temperature T_m° the temperature

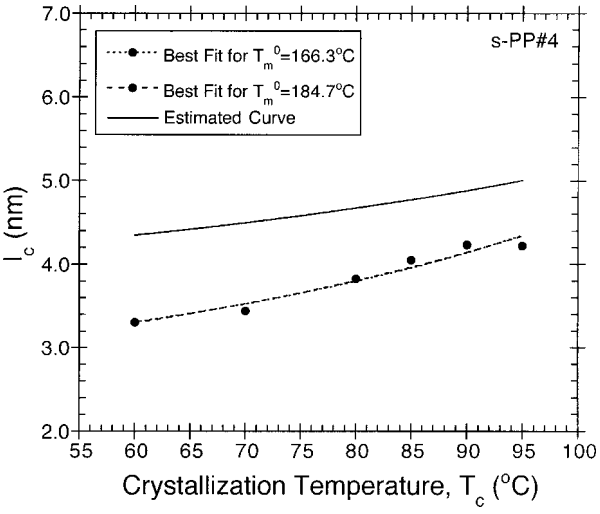

Figure 9. Plot of lamellar thickness l_c as a function of the crystallization temperature T_c (without the data points at T_c=30, 40 and 50 °C). The dotted and dashed lines are the best fits of the experimental data (●) according to eqn (13) when T_m° is taken as 166.3 °C and 184.7 °C, respectively. The solid line is the estimated curve calculated according to eqn (13) using $\sigma_e^1 \approx \sigma_e^{GT} = 57.8$ mJ m^{-2}, $T_m^\circ = 184.7$ °C, $\Delta H_f^\circ = 4.6$ kJ mol^{-1} and a=2.34.

dependence of the initial lamellar thickness l_c^* for s-PP can be written as

$$l_c^* = \frac{2248.2}{166.3 - T_c} + 11.9 \qquad (r^2 = 0.972) \qquad (15)$$

or

$$l_c^* = \frac{3321.7}{184.7 - T_c} + 6.3 \qquad (r^2 = 0.975) \qquad (16)$$

if choices of $T_m^\circ = 166.3\,^\circ\mathrm{C}$ and $184.7\,^\circ\mathrm{C}$ are used, respectively. It should be noted that the units of l_c^* and T_c in eqns (15) and (16) are Å and °C, respectively. Instead, if we are to estimate the temperature dependence of the initial lamellar thickness l_c^* for s-PP based on theoretical ground (ie $D_1 = 2\sigma_e^1 T_m^\circ / \Delta H_f^0$ and $D_2 = 2\sigma_e^1 a / \Delta H_f^0$, where $\sigma_e^1 \approx \sigma_e^{GT} = 57.8\,\mathrm{mJ\,m^{-2}}$, $T_m^\circ = 184.7\,^\circ\mathrm{C}$, $\Delta H_f^0 = 4.6\,\mathrm{kJ\,mol^{-1}}$ and $a = 2.34$), we arrive at the following equation:

$$l_c^* = \frac{2100.7}{184.7 - T_c} + 26.6 \qquad (17)$$

where the units of l_c^* and T_c are Å and °C, respectively. The estimated temperature dependence of the initial lamellar thickness l_c^* for s-PP based on eqn (17) is also plotted in Fig 9 as the solid line; evidently, the estimation overpredicts the size of the initial lamellar thickness l_c^* at a given crystallization temperature. This discrepancy will be a subject of further investigation.

CONCLUSIONS

WAXD, SAXS and DSC techniques were employed to investigate the lamellar morphology and subsequent melting behaviour of s-PP samples isothermally crystallized at temperatures ranging from 30 to 95 °C. All the samples investigated were found to crystallize in the high temperature, orthorhombic limit-disordered form I. The degree of crystallinity χ_c^{WAXD}, the long period L_B, the lamellar thickness l_c and the melting temperature T_m were all found to increase with increasing crystallization temperature. The equilibrium enthalpy of fusion ΔH_f^0 was found to be $109.3 \pm 0.5\,\mathrm{J\,g^{-1}}$ or ca. $4.6\,\mathrm{kJ\,mol^{-1}}$. The Gibbs–Thomson extrapolation suggested approximate values of the equilibrium melting temperature T_m^{GT} and the basal interfacial free energy σ_e^{GT} of 166.3 and $57.8\,\mathrm{mJ\,m^{-2}}$, respectively, while the LHW and NLHW extrapolation methods gave approximate values of the equilibrium melting temperature T_m^{LHW} and T_m^{NLHW} of 142.8 °C and 184.7 °C, respectively. Finally, the equilibrium melting temperature of a perfect s-PP sample $(T_m^\circ)_{100\%}$ was estimated to be about 199.2 °C.

ACKNOWLEDGEMENTS

We should like to thank Dr Joseph Schardl of Fina Oil and Chemical Co, Dallas, Texas, for supplying the s-PP resins used in this study, and Dr Roger A Phillips and his co-workers of Montell USA, Inc, Elkton, Maryland, for performing molecular characterizations of the resin. The research at Oak Ridge was sponsored in part by the US Department of Energy, under contract no DE-AC05-OOOR22725 with the Oak Ridge National Laboratory, managed by the UT-Battelle, Lld. Lastly, constructive comments made by the reviewers are greatfully acknowledged.

REFERENCES

1 Natta G, Pasquon I, Corradini P, Peraldo M, Pegoraro M and Zambelli A, *Rend Aocad Naz Lincei* **28**:539 (1960).
2 Natta G, Pasquon I and Zambelli A, *J Am Chem Soc* **84**:1488 (1962).
3 Ewen JA, Johns RI, Razavi A and Ferrara JD, *J Am Chem Soc* **110**:6255 (1988).
4 Rodriguez-Arnold I, Bu Z and Cheng SZD, *J Macromol Sci Rev Macromol Chem Phys* **C35**:117 (1995).
5 Wheat WR, *SPE-ANTEC Proc*, pp 2275 (1995).
6 Schardl I, Sun I, Kimura S and Sugimoto R, *J Plast Film Sheeting* **12**:157 (1996).
7 Sun I, Shamshoum E and DeKunder G, *SPE-ANTEC Proc*, pp 1965 (1996).
8 Wheat WR, *SPE-ANTEC Proc*, pp 565 (1997).
9 Gownder M, *SPE-ANTEC Proc*, pp 1511 (1998).
10 Sura RK, Desai P and Abhiraman AS, *SPE-ANTEC Proc*, pp 1764 (1999).
11 Rodriguez-Arnold J, Zhang A, Cheng SZD, Lovinger AJ, Hsieh ET, Chu P, Johnson TW, Honnell KG, Geerts RG, Palackal SJ, Hawley GR and Welch MB, *Polymer* **35**:1884 (1994).
12 Supaphol P, Hwu JJ-J, Phillips PJ and Spruiell JE, *SPE-ANTEC Proc*, pp 1759 (1997).
13 Supaphol P and Spruiell JE, *J Appl Polym Sci* **75**:44 (2000).
14 Rodriguez-Arnold I, Bu Z, Cheng SZD, Hsieh ET, Johnson TW, Geerts RG, Palackal SJ, Hawley GR and Welch MB, *Polymer* **35**:5194 (1994).
15 Supaphol P and Spruiell JE, *Polymer* **41**:1205 (2000).
16 Bu Z, Yoon Y, Ho R-M, Zhou W, Jangchud I, Eby RK, Cheng SZD, Hsieh ET, Johnson TW, Geerts RG, Palackal SJ, Hawley GR and Welch MB, *Macromolecules* **29**:6575 (1996).
17 Supaphol P and Spruiell JE, *J Appl Polym Sci* **75**:337 (2000).
18 Wignall GD, Lin J-S and Spooner S, *J Appl Crystallogr* **23**:241 (1990).
19 Russell TP, Lin J-S, Spooner S and Wignall GD, *J Appl Crystallogr* **21**:629 (1988).
20 Corradini P, Natta G, Ganis P and Temussi PA, *J Polym Sci* **C16**:2477 (1967).
21 Lotz B, Lovinger AJ and Cais RE, *Macromolecules* **21**:2375 (1988).
22 Lovinger AJLotz B and Davis DD, *Polymer* **31**:2253 (1990).
23 Chatani Y, Maruyama H, Noguchi K, Asanuma T and Shiomura T, *J Polym Sci* **C28**:393 (1990).
24 Lovinger AJ, Davis DD and Lotz B, *Macromolecules* **24**:552 (1991).
25 Chatani Y, Maruyama H, Asanuma T and Shiomura T, *J Polym Sci Polym Phys* **29**:1649 (1991).
26 Lovinger AJ, Lotz B, Davis DD and Padden FJ, *Macromolecules* **26**:3494 (1993).
27 De Rosa C and Corradini P, *Macromolecules* **26**:5711 (1993).
28 Auriemma F, De Rosa C and Corradini P, *Macromolecules* **26**:5719 (1993).
29 De Rosa C, Auriemma F and Corradini P, *Macromolecules* **29**:7452 (1996).
30 De Rosa C, Auriemma F and Vinti V, *Macromolecules* **30**:4137 (1997).
31 Lovinger AJ and Lotz B, *J Polym Sci Polym Phys* **35**:2523 (1997).
32 Auriemma F, De Rosa C, Ruiz de Ballesteros O, Vinti V and Corradini P, *J Polym Sci Polym Phys* **36**:395 (1998).
33 De Rosa C, Auriemma F, Vinti V, Grassi A and Galimberti M, *Polymer* **39**:6219 (1998).

34 De Rosa C, Auriemma F and Vinti V, *Macromolecules* **31**:7430 (1998).
35 De Rosa C, Talarico G, Caporaso L, Auriemma F, Galimberti M and Fusco O, *Macromolecules* **31**:9109 (1998).
36 Supaphol P and Spruiell JE, *J Appl Polym Sci*, submitted for publication.
37 Hoffman JD, Davis GT and Lauritzen Jr JJ, in Treatise on Solid State Chemistry; Vol 3, Ed by Hannay NB, Plenum Press, New York, Chapter 7 (1976).
38 Hoffman JD and Weeks JJ, *J Res Natl Bur Stand* **A66**:13 (1962).
39 Schmidtke J, Strobl G and Thurn-Albrecht T, *Macromolecules* **30**:5804 (1997).
40 Hauser G, Schmidtke J and Strobl G, *Macromolecules* **31**:6250 (1998).
41 Hugel T, Strobl G and Thomann R, *Acta Polym* **50**:214 (1999).
42 Marand H, Xu J and Srinivas S, *Macromolecules* **31**:8219 (1998).
43 Alamo RG, Viers BD and Mandelkern L, *Macromolecules* **28**:3205 (1995).
44 Xu J, Srinivas S, Marand H and Agarwal P, *Macromolecules* **31**:8230 (1998).
45 Lauritzen Jr JI and Passaglia E, *J Res Natl Bur Stand* **A71**:261 (1967).
46 Hoffman JD and Miller RL, *Polymer* **38**:3151 (1997).